

# We are IntechOpen, the world's leading publisher of Open Access books Built by scientists, for scientists

6,900

Open access books available

185,000

International authors and editors

200M

Downloads

Our authors are among the

154

Countries delivered to

TOP 1%

most cited scientists

12.2%

Contributors from top 500 universities



WEB OF SCIENCE™

Selection of our books indexed in the Book Citation Index  
in Web of Science™ Core Collection (BKCI)

Interested in publishing with us?  
Contact [book.department@intechopen.com](mailto:book.department@intechopen.com)

Numbers displayed above are based on latest data collected.  
For more information visit [www.intechopen.com](http://www.intechopen.com)



## Analytical Compact Models

Bruno Allard and Hervé Morel

*Université de Lyon, INSA Lyon, AMPERE-Lab, Villeurbanne, France*

### 1. Introduction

The virtual prototyping of power electronic converters is considered here. Virtual prototyping is now an important challenge in the context of integration of power systems. If semiconductor devices are considered as the levellers of significant advances in power converters, it is commonly admitted that the next leveller of advances is related to the design methods. The design methods ambition to deliver a satisfying product with the first prototype as a prototype of a power converter is expensive.

Differences in virtual prototyping acceptance may be foreseen depending on the level of integration. On the one hand VLSI power management requires methodologies and models in the framework of integrated circuit tools. The dedicated tools seem to dictate the nature of the models and of the design flow. On the other hand the design of a mechatronic system could rely on a wider range of models and methodologies depending on the background of the involved engineer. In fact the development of virtual prototyping methodologies try to provide a systematic approach to the different steps involved in the emergence of a product. Depending on the complexity of a given system, all or parts of the models and analyses will be solicited.

The idea is that a simple step-down DC/DC converter represents a similar design problem whether a 1 W monolithic IC is required or a 100 W discrete-board converter inside a car mechatronic-item is specified. The common part in the design process of these two seemingly different converters concerns the early stage of virtual prototyping, namely the pre-design. Fig. 1 details the macro-steps in the design flow of a power converter, but the idea is applicable to a mechatronic device. Pre-design covers the early steps in the design flow.

Other steps in the design process will involve hard technology constraints, what will affect the complexity level of some models but design analyses remain essentially the same whatever the level of integration. These intermediate steps in the design process refer to what is practically known as design, what is in essence to choose devices and to optimize circuits. When device and circuits have been globally optimized, next steps concern the geometrical and physical assembly of these devices into a converter. Additional physical phenomena appear that require dedicated tools and models to complete the optimization of the power converter. The final steps in the design process concern the virtual physical verification of the system. The technology constraints and the geometrical size of the system, adding the power level, dictate different approaches for the analyses to be carried out. The latter verification efforts are in relation to the system specifications and receipt.

The early stages of virtual prototyping are the most risky as the possible cost of an error in any choice will continually rise with subsequent design steps. The chapter details several necessary models for the early stages in virtual prototyping, namely the system-level analyses in Fig. 1.

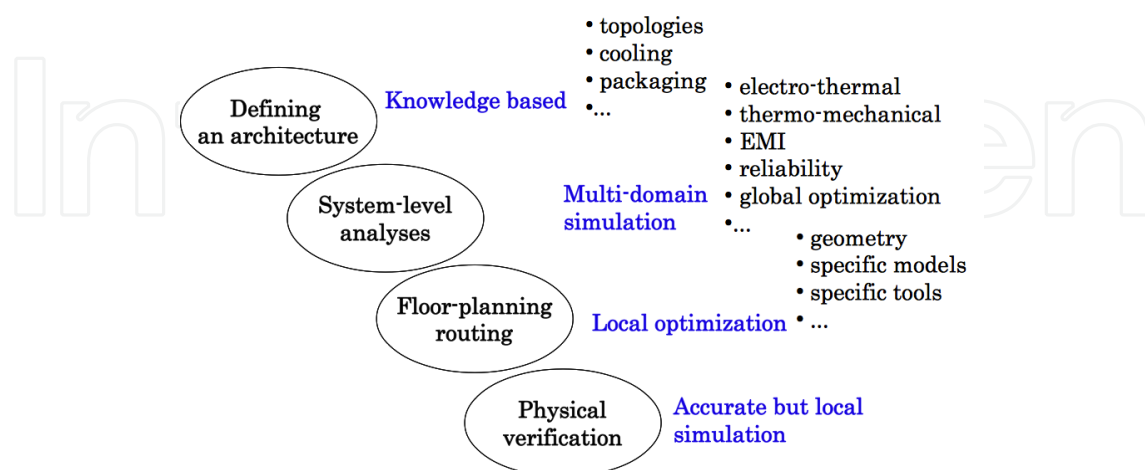


Fig. 1. Schematic of a classical design flow for a power converter with related macro-steps

## 2. Analytical compact models

Facing the specifications of a power converter, either highly integrated or in relation with a hybrid technology, the electronic engineer has to make a choice of architecture (see Fig. 1). The architecture is a response to the main functionality, i.e. the kind of energy process operated by the required converter. The architecture involves components and operation principles. Unfortunately the specified converter must offer performances in a wide range of operating conditions. Cost, power density, efficiency and reliability are generally the hard performances to address. A satisfying level of trade-off cannot be settled without a proper methodology. The methodology is based on databases, models of components and optimization routines.

When best candidate architectures have been identified, the design goes a step further to confirm various quantities as current, voltage and temperature ratings. Evaluation regarding Electromagnetic compatibility (EMC) is generally a troublemaker. EMC is correlated to some point with efficiency and a second set of optimization against power density and cost will confirm or infirm the possibility of architectures. When one architecture is validated at this step, a practical design-process begins, as it is known for decades. This practical design step depends on the technology and field-related tools are considered. If EMC, efficiency and other considerations do not permit to validate the foreseen architecture from the system elaborated by the pre-design, it is necessary to relax the specifications in any way. It is then mandatory to run the pre-design and the confirmation design step as fast as possible to limit the risk in the subsequent design steps. As a tremendous number of architectures may be considered, it is necessary to provide models dedicated to pre-design and the confirmation design step.

A power converter circuit is made of many devices. Many abstraction models have been developed and detailed in literature (Middlebrook, 1976), (Cùk, 1977), (Krein, 1990), (Lee, 1985), (Sanders, 1991), (Smedley, 1994), (Ben-Yaakov, 1995), (Lai, 1995), (Maksimovic, 1998),

(Xu, 1994), (Olivier, 2000). A functional view of a power converter has been proposed as the so-called average model. The abstraction is to get rid of the switching process. In another way, the goal is to keep only the most significant time-constants in the power converter from control point of view. Fig. 2 gives an idea of the spread of time-constants of physical phenomena in a power converter.

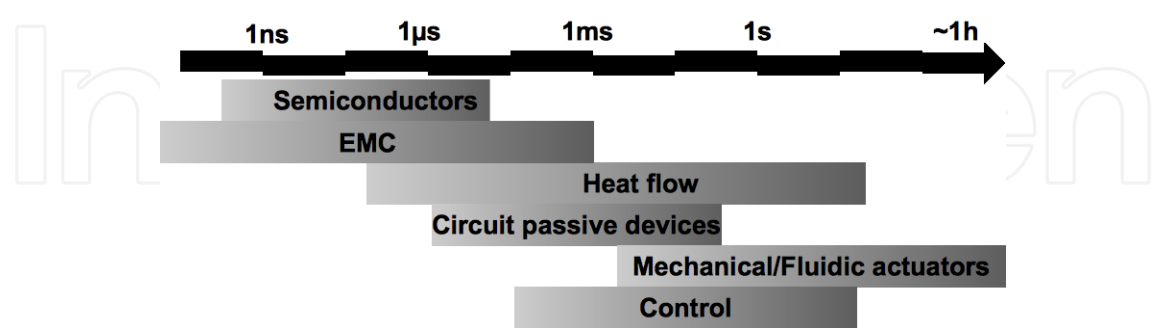


Fig. 2. Repartition of time-constants of physical phenomenon in a power converter

In early 70's appeared most of the power converter architectures as known today. The circuit simulators at the time were sufficiently developed for the field-engineer to detect that basic discrete devices would not be sufficient. The integration time-step in a circuit simulator is dictated by the smallest time-constant. Unfortunately the field-engineer is firstly interested by long-term simulation. The simulation cost is then unaffordable and the necessity for more efficient models of converters emerged. The development of such models has required a tremendous effort and more than hundred thousands of papers have been published on the topic. The name of averaged models comes from the idea to look at the power converter on the basis of the switching period and to eliminate whatever phenomenon exhibiting a time-constant lower than this switching period. Nowadays such models are qualified of "compact models". They are dedicated to system-level analyses. Fig. 3 lists some of the system-level analyses mentioned in Fig. 1. The figure shows that the compact models useful for a given analysis will cover more than one physical domain and a large spectrum of time-constants.

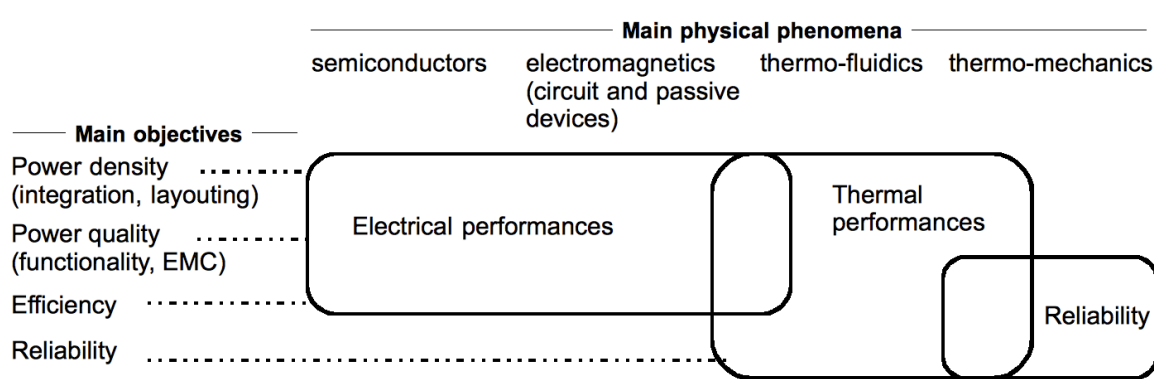


Fig. 3. Relation between system-level analyses and physical phenomena

The average model is mainly used to build feedback loops. One method called the state-space averaging method has been used for decades. Unfortunately the latter method does not apply easily to resonant converters and does not accept non-linear terms as power losses or delays between control signal and power flow. Contribution to EMC is not possible.

Probably this explains that EMC issues are generally considered at the end of the design process and the cost may be significant in additional filters or reduced performances. The power electronic engineer has been dealing with the average model of the converter at hand but he needed to add some view about power losses and temperature. Equivalent electrical models of thermal networks are popular and considered in most approaches. The manufacturer of a thermal system generally gives a practical thermal model of its product or at least an abacus of the so-called thermal impedance of the thermal path. Unfortunately a thermal network is based on the association of thermal effects and/or products and the addition of the practical models – thermal impedances- is not accurate enough. Restricting the analysis to steady-state operation is not sufficient to obtain pertinent evaluations with these practical models. The need for light but accurate models of a thermal network has given rise to methodologies to build so-called compact thermal models. A compact thermal model is a global behavioural model taking power losses in the system as inputs and evaluating specific temperatures inside the systems. These specific temperatures are mostly averaged operating temperatures of the power semiconductor devices and power passive devices. The term of junction temperature is improperly used here.

The chapter wishes to detail methods to build efficiently compact models for the average representation of converters but including power losses. EMC contributions can also be added and compact models of thermal network must be considered to attain electro-thermal simulation.

The proposed compact models come as state-space models and may be used in any simulator providing an entry language. Standard languages are available to distribute such models like VHDL-AMS, IEEE 1076.1.

A hardware description language is unfortunately not a guide for efficient modelling. Alternatively bond graphs are known for decades and have been provided for modelling the dynamics of multi-domain systems. Bond graphs are a framework for graphical representation but implement many methods like the causality analysis. An original extension of the causality analysis was provided to build compact average models. An extension to include power losses is presented here. Contribution to EMC was a recent addition to the method. Examples will be presented to illustrate the detail of the methods.

Bond Graphs are covered in many books and papers. A short description is provided at the end of the chapter to enable the reader to follow the presentation without pre-requisites.

### 3. The algebraic causality analysis

This introductory section requires the prior reading of appendices. ACA is a systematic procedure that enhances the causality analysis of a bond graph. It supports then the systematic compact model calculation.

Karnopp and Rosenberg in (Karnopp, 1975, 1990) describe a graphical causality analysis that applies only to bond graphs made of linear elementary components (see section 13). This graphical method is limited in the case of bond graphs that incorporate more complex components. Many electronic devices constitute complex components described with large state-space models including non-linear functions. It must be recalled here that Bond Graphs must be considered as a building framework to derive the constitutive equations of the model of a system. These equations are to be handled by a simulator and nowadays VHDL-AMS is an example of language suitable to perform this task of model handling (Pecheux, 2005). It is presented here an extension of the original causality analysis, called

initially Algebraic Causality Analysis (Allard, 1997a). The purpose is to provide a software-compatible algorithm. ACA considers that state-space models of variable causality represent the components of a bond graph. ACA uses a graphical representation that separates the knowledge of the causality for flow variables and the effort variables.

The graphical representation is listed in Table 6 for non-varying causality components. A power switch with a gate control gives an example of varying causality. When the gate control is not activated (like in a power MOSFET or IGBT), the power switch is in off state and the causality of its power bond is to enforce the flow variable: the switch is a source of null-current. When the gate control is activated, the power switch is equivalent to a source of null-voltage in the ideal case, and the causality is related to the effort variable. This particularity is illustrated in next section.

### 3.1 Systematic algorithm

The algorithm is applied through the following steps:

1. Apply the causality of sources ( $Se$ ,  $Sf$ ) including varying-causality elements
2. Apply the causality of storage elements assuming the integral causality. This also applies to any state-space element.
3. Propagate the causality knowledge through junctions, transformers, gyrators and resistors.
4. Iterate step 3 until the following situation:
  - All causal strokes are drawn without conflict: the bond graph is causal (best case)
  - A conflict of causality appears during the iteration: causality knowledge concerns a variable already known (causal stroke already drawn). It is the case of a redundant equation.
  - It remains a bond without a causal stroke. There is a non-determination of one variable.
  - An example of case (i) above is given by the series RLC circuit in Fig. 28(c). The algorithm application is detailed in Table 4.

### 3.2 Application to a faulty bond graph

In the example of Fig. 4, the two capacitors connected in parallel lead to a causality fault at the 0-junction. Choosing one of the capacitor in derivative causality solves the causality (see Table 6). The circuit model is then a DAE of index 1.

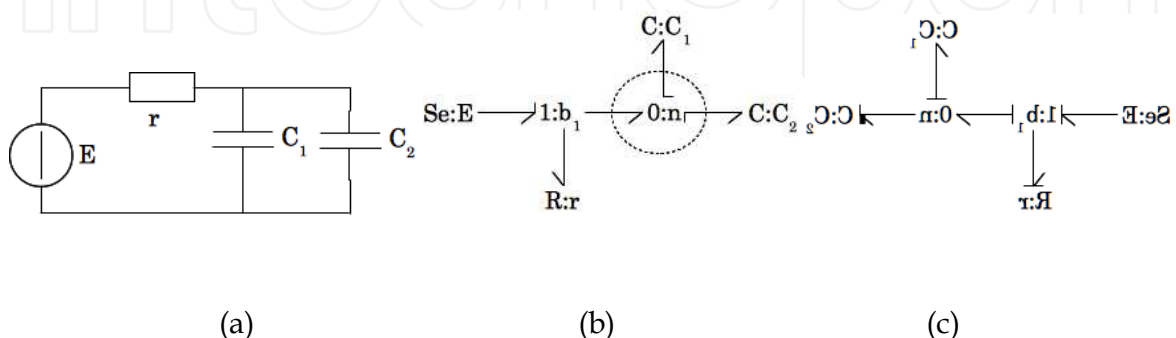


Fig. 4. Simple electrical circuit (a) leading to a causality fault (b), solved by a derivative causality (c).



	Initial bond graph
	1 - Causality of sources Se: the effort variable is known and the half-stroke for effort variable is added. The half stroke is placed below the half-arrow by convention (see Table 6).
	2 - Causality of state-space components (C, I ... ) in integral causality. The inductance model yields the value of the current, i.e. the flow variable. A half-stroke is placed on the side of the half-arrow.
	2 - Causality of state-space components (C, I ... ) in integral causality. The capacitor model yields the voltage and an half-stroke indicates the effort variable causality.
	3 - Propagate the causality through junctions, transformers and resistors. The flow variable common to all bonds of the 1-junction is dictated by the inductance. This knowledge is propagated with 3 half-strokes.
	3 - Propagate the causality through junctions, transformers and resistors. The resistor model has two forms. As the flow variable is known, one form dictates the voltage, i.e. the effort variable and a half-stroke is added accordingly.
	4 - iterate step 3 3 - Propagate the causality through junctions, transformers and resistors. The 1-junction model enables to compute the voltage across the inductance as the other voltage drops are known from the other bonds.

Table 1. Application of ACA algorithm on a causal bond graph

A second example is a simple chopper circuit as in Fig. 5. The model in Equation 1 represents a power MOSFET and the model in Equation 2 represents a power diode (Morel, 2001).

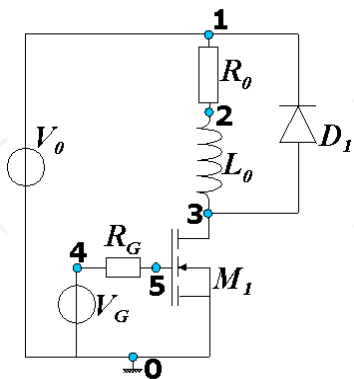


Fig. 5. Simple chopper circuit

ACA is applied step by step (Table 2). ACA terminates with clause (iii) and the current  $i_A$  and  $i_E$  are not determinate. A circuit simulator gives a result of such a model but experiment does not confirm the result. It is a well-known problem: the model lacks a parasitic inductance at node 1 in Fig. 5 that splits the power supply current between the inductance and the power diode. ACA helps here to exhibit lack in the model that the Nodal Analysis does not detect.

Bond graph	Comments	Equation
	Initial Bond graph	State-variables are $Q_g, Q_j$ charges in MOSFET. $Q_d$ charge in diode junction $\Phi$ flux in inductance
	1- causality of sources $Se :E$ and $Se :G$	$v_E = E, v_G = G(t)$
	2 - causality of state-space elements $I :L_0,$ MOSFET M and diode D	$i_L = \frac{\phi}{L}$ $v_{DS} = g_4(Q_j, Q_G)$ $v_{GS} = g_3(Q_j, Q_G)$ $v_D = g_1(Q_D)$



Bond graph	Comments	Equation
	3-Propagation of causality  1-junction linked to MOSFET	$v_N = v_E - v_{DS}$
	3-Propagation of causality  internal 0-junction	Similar voltage drop across all 0-junction bonds
	Causality fault at 1-junction linked to diode D  clause (ii): variable already known	The causality fault corresponds to the constraint: $v_N + v_D = 0$
	3-Propagation of causality  1-junction linked to L0 and R	$i_L$ is the current in each bond of the 0-junction
	3-Propagation of causality  element R	$v_R = R \cdot i_L$ $v_L = v_N - v_R$
	3-Propagation of causality  1-junction linked to Se:G and element R	$v_{R_G} = v_G - v_{GS}$ $i_G = \frac{v_{R_G}}{R_G}$  $i_G$ is the current in each bond of the 1-junction

Table 2. ACA applied to the circuit in Fig. 5

$$\begin{aligned}\frac{dQ_G}{dt} &= i_G \rightarrow \text{gate charge} \\ \frac{dQ_J}{dt} &= i_{DS} - g_2(Q_J, Q_G) \rightarrow \text{Miller capacitance} \\ v_{GS} &= g_3(Q_J, Q_G) \rightarrow \text{gate voltage} \\ v_{DS} &= g_4(Q_J, Q_G) \rightarrow \text{drain voltage}\end{aligned}\tag{1}$$

$$\begin{aligned}\frac{dQ_D}{dt} &= i - i_D(Q_D) \\ v_D &= g_1(Q_D)\end{aligned}\tag{2}$$

4. Average models of ideal non-resonant converters

Many methods to build average models of power converters have been published but with two major limitations so far (Allard, 1997b, 1999). On one hand the methods handle only ideal representation of non-resonant converters. On the other hand the methods take the converter as a all and do not differentiate the time-constants to be averaged. The proposed building procedure is then developed on the simplest example of DC/DC converter. The procedure has been translated into a computer program and integrated inside commercial simulators. Results are extrapolated to any non-resonant ideal DC/DC converter. The building procedure is based on ACA and switching bond graphs, i.e. made of elements of varying causality (Ammous, 2003). The ideal power switches are illustrated in Fig. 6. A power converter that incorporates such ideal switches is affected by the changes in causality: this leads to the so-called topologies of the converter. These are seen here as changes in the assignment of the causality. Fig. 7 illustrates two causality assignments for a basic step-down DC/DC converter.

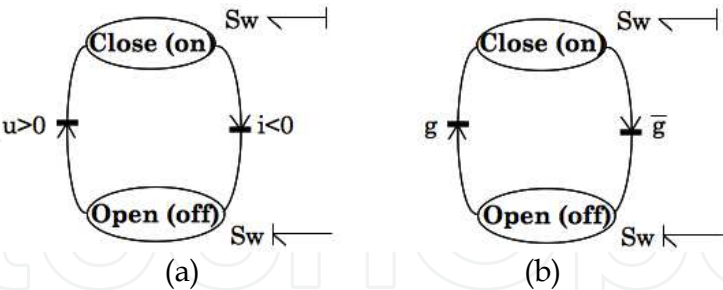


Fig. 6. Ideal natural switch (a) and ideal controlled switch (b)

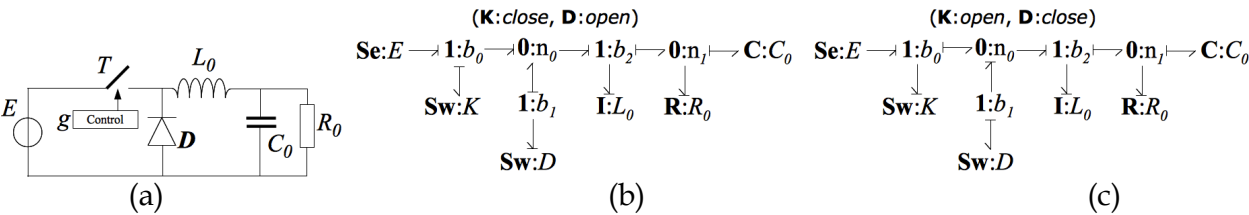


Fig. 7. Ideal step-down DC/DC converter (a) with two causality assignments depending on the state of the power switches (b) and (c).

It is considered now on that the switching period of a DC/DC power converter is always smaller than the time-constants of the passive filter components. The power switches, based on the control signals, define a sequence of causality assignments in the bond graph of the converter. The simplest sequence is generally called the continuous conduction mode (the current never reaches a null value in the inductance in Fig. 7(a)). This sequence comprises two causality assignments. A Petri Network is a convenient tool to picture a sequence. Fig. 8 gives two sequences for the converter in Fig. 7(a).

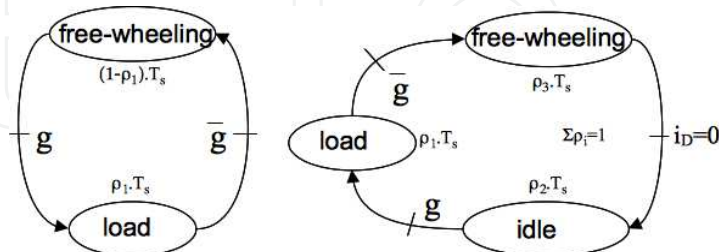


Fig. 8. Two typical causality assignment sequence for a DC/DC converter

The algorithm to build the average model of a DC/DC converter requires knowing the converter architecture (including control signals) and a given sequence of operation. Each sequence of operation requires the derivation of an average model: hence the interest for a systematic method. Six steps have identified.

1. Identification of the switching block: it is made of the all the components which causality changes over the sequence of causality assignment. The resistor connected to an internal junction of the switching block must be included as well.

*The bond graph of the ideal buck-boost architecture in Fig. 9 suffers two causality analyses for the continuous conduction mode sequence (Fig. 10). The switching block is then {M, l1, n1, l2, D}*

2. Identification of the external variables of the switching block: these are the effort and flow variables of the bonds external to the switching block except the control signals.

*Fig. 11 pictures the external bonds to the switching block and the external variables #1( $i_1$ ,  $v_1$ ), #2( $i_L$ ,  $v_L$ ) et # ( $i_2$ ,  $v_2$ )*

3. Identification of the input variables to the switching block: these are the variables known from the causality of the components external to the switching block.

*As pictured in Fig. 11, the external components of the switching block dictate the following variables:  $v_1$  on bond #1,  $i_L$  on bond #2 and  $v_2$  on bond #3.*

4. Simplification of the bond graph: the external bonds to the switching variables are replaced by sources of same causality as the input variables.

*The external components of the bond #1 are replaced by a voltage source, a current source for bond #2 and a voltage source for bond #3.*

5. Expression of the output variables of the switching block

*In "free-wheeling" state of the sequence of causality assignment (M: off, D: on),  $i_1=0$ ,  $v_L=v_2$  and  $i_2=i_L$ . In "load" state (M: on, D: off),  $i_1=i_L$ ,  $v_L=E$  and  $i_2=0$ .*

6. Computation of the average model by the weight-based averaging of the output variables with respect to the duration of the related causality assignment in the switching sequence. Three typical cases appear:

- a. Output variables do not depend on state-variables: immediate result as the variable is independent of time.

*The duty-cycle for the power switch M is  $\rho$ , and it comes the average values:  $\langle i_1 \rangle = \rho \cdot I_L$ ,  $\langle v_L \rangle = \rho \cdot V_1 - (1 - \rho) \cdot V_2$ ,  $\langle i_2 \rangle = (1 - \rho) \cdot I_L$ . The bond graph in Fig. 12 may be drawn as the previous equations are related to MTF elements with appropriate ratio ( $f_1=m.f_2$ , see Fig. 25).*

- b. Output variables depend on state-variables through inferable functions: an analytical solution is possible
- c. Output variables depend on state-variables through non-linear functions: a numerical integration is necessary.

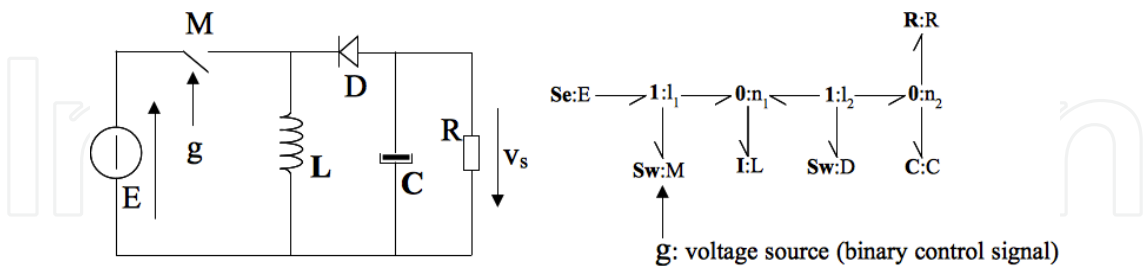


Fig. 9. Ideal buck-boost converter and associated bond graph

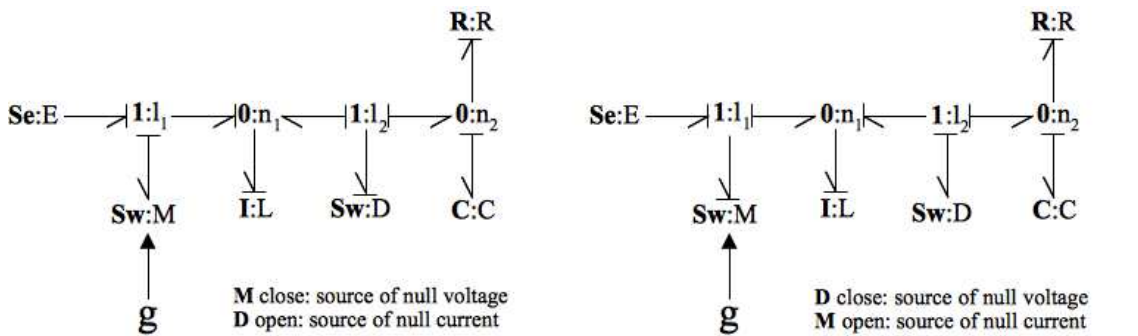


Fig. 10. The two causality assignments in the sequence of in continuous conduction mode of the ideal buck-boost converter

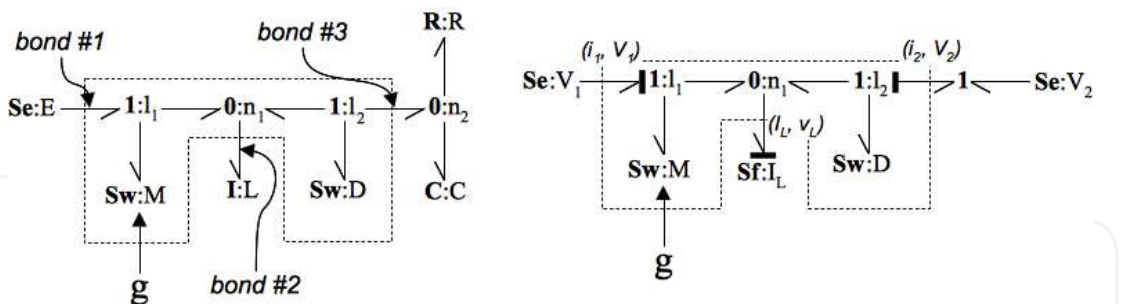


Fig. 11. Steps 3 and 4 of the algorithm

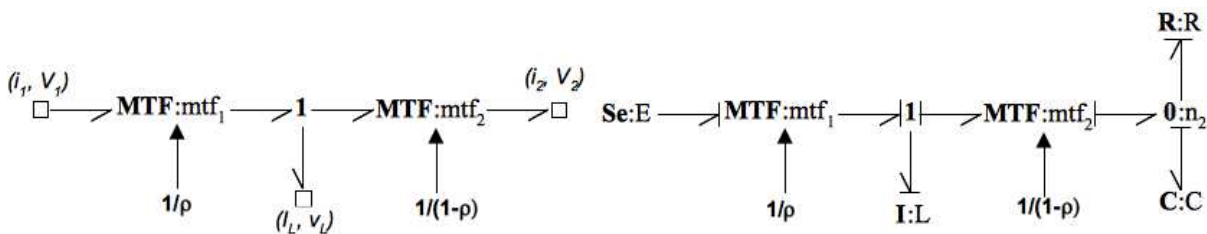


Fig. 12. Average model of the switching block and average model of the ideal buck-boost converter.

Fig. 12 enables to draw the bond graph of the average model of the ideal buck-boost. This model has been obtained in a systematic manner. The EDO of the average-model state-space equation is then obtained in a straightforward manner.

$$\frac{d}{dt} \begin{bmatrix} i_L \\ v_C \end{bmatrix} = \begin{bmatrix} 0 & \frac{1-\rho}{L} \\ \frac{1-\rho}{C} & -\frac{1}{RC} \end{bmatrix} \begin{bmatrix} i_L \\ v_C \end{bmatrix} + E \begin{bmatrix} \frac{\rho}{L} \\ 0 \end{bmatrix}$$

(3)

5. Average models of ideal resonant converters

The building procedure is now applied to a simple resonant converter. It is a major contribution to the state of the art as none of the previous methods (based on the Generalized Stat-Space Averaging Method) were able to process a change in state-space variables. The above-mentioned algorithm is applied in a straightforward manner. It is considered the example of the ideal ZVS-boost converter (Fig. 13(a)) in continuous conduction mode (Fig. 13(b)).

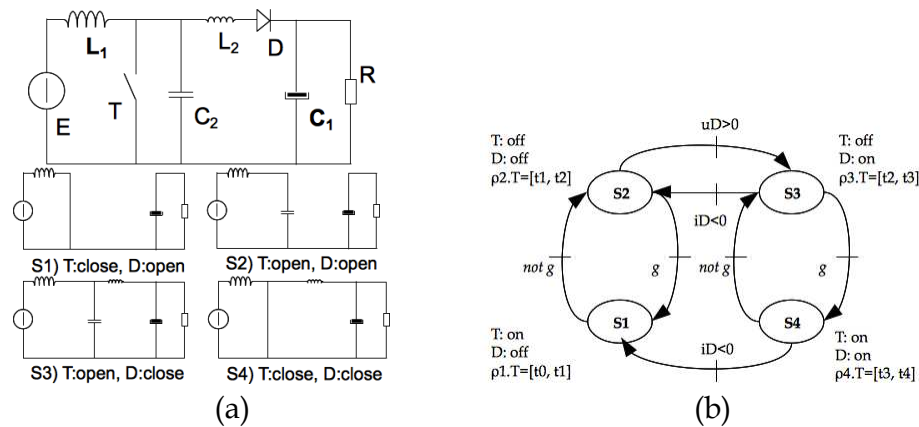


Fig. 13. Ideal ZVS-boost converter in continuous conduction mode (a) and related sequence of causality assignment (b)

At the end of step 4, it comes the simplified bond graph in Fig. 14(b). The switching block is identified as {T, D, C2, L2, n1, l2} with 2 external bonds. The input variables are I1 and V2.

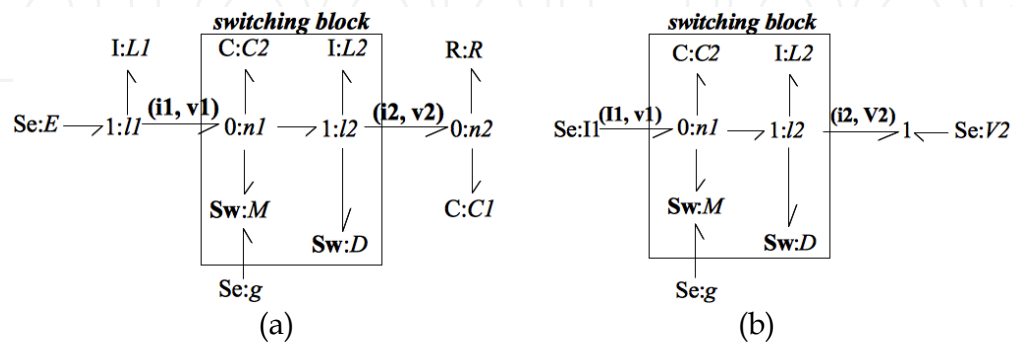


Fig. 14. Title of figure, left justified

Step 5 is to express the output variables of the switching block (v1, i2) in the four cases of causality assignment. The results are summarized in Table 3. The computation of the input

variables implies that causal bond graphs be obtained. This leads to consider derivative causality for the inductor L2 in states S1 and S2, and for the capacitor C2 in state S1 and S4. The Algebraic Causality Analysis helps finding systematically the latter considerations. It is this level of details that makes the difference with past methods to build average models and explains their limitations with regard to resonant architectures of power converters.

¶State S1	State S2	State S3	State 4
T: on, D: off L2: derivative <sup>1</sup> C2: derivative	T: off, D: off L2: derivative C2: integral <sup>2</sup> (Q2)	T: off, D: on L2: integral (φ2) C2: integral (Q2)	T: on, D: on L2: integral (φ2) C2: derivative
$v_1 = 0$ $i_2 = 0$	$v_1 = \frac{Q_2}{C_2}$ $i_2 = 0$ $\frac{dQ_2}{dt} = I_1$	$v_1 = \frac{Q_2}{C_2}$ $i_2 = \frac{\phi_2}{L_2}$ $\frac{dQ_2}{dt} = I_1$ $\frac{d\phi_2}{dt} = \frac{Q_2}{C_2} - V_2$	$v_1 = 0$ $i_2 = \frac{\phi_2}{L_2}$ $\frac{d\phi_2}{dt} = -V_2$

Table 3. Development of step 5 of the algorithm applied to the ideal ZVS-boost converter.

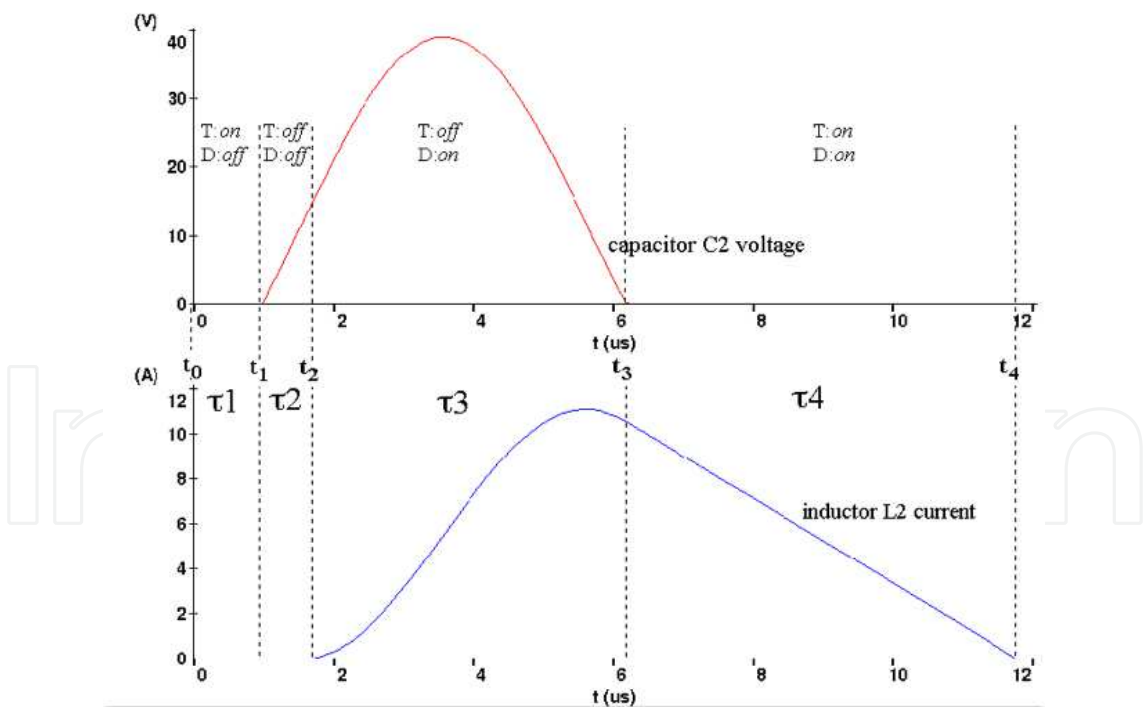


Fig. 15. Simulation of the simplified bond graph in Fig. 14(b)

<sup>1</sup> derivative causality: no state variable, i.e. a DAE model, see Table 6  
<sup>2</sup> integral causality: normal state variable model (namely the charge Q2 for the capacitor and the magnetic flux φ2 for the inductor), see Table 6



Table 3 in fact summarizes the model of the simplified bond graph in Fig. 14(b). A simulation of this model gives the result in Fig. 15. The zero-voltage switching of the converter is clearly illustrated. Step 6 concerns the expression of the average values of the switching block output variables ( $v_1$ ,  $i_2$ ) over the sequence in Fig. 13(b). The respective duration of each state concurs to the switching period  $T_s$ . Formal mathematical manipulations leads to Equation 4. The common way to represent this average model is to consider a MTF element which ratio would be in fact  $\rho_1$ . The average model of the ideal ZVS-boost converter is obtained when adding the external components of the switching block to the MTF element.

$$\left\{ \begin{aligned} \langle i_2 \rangle &= \frac{1}{T_s} \left[ \frac{I_1 \cdot \alpha}{\omega} + C_2 \cdot V_2 + \frac{L_2 \cdot I_1^2}{2 \cdot V_2} \cdot (1 - \cos \alpha)^2 \right] \\ \langle v_1 \rangle &= \frac{1}{T_s} \left[ \frac{C_2 \cdot V_2^2}{2 \cdot I_1} + \frac{V_2 \cdot \alpha}{\omega} + L_2 \cdot I_1 \cdot (1 - \cos \alpha) \right] \end{aligned} \right\} \text{ with } \left\{ \begin{aligned} T_s &= \frac{1}{1 - \rho_1} \left[ \frac{C_2 \cdot V_2}{I_1} + \frac{\alpha}{\omega} + \frac{L_2 \cdot I_1}{V_2} \cdot (1 - \cos \alpha) \right] \\ \omega &= \sqrt{\frac{1}{L_2 \cdot C_2}} \\ \sin \alpha &= \frac{-V_2}{I_1} \cdot \sqrt{\frac{C_2}{L_2}} \end{aligned} \right. \quad (4)$$

## 6. Non-linear average models

So far the construction of average model of converters has been applied to ideal architecture. Two contributions have been demonstrated in previous sections: it is a systematic procedure, providing the algebraic causality analysis, and it applies equally to resonant converters. As mentioned in Fig. 1, ideal average models are only useful in early time of the virtual prototyping. It is necessary to incorporate the evaluation of power losses in the average models. Devices in static and transient operations generate power losses. Steady-state power losses are easy to incorporate as they depend only on the current and voltage across the devices. Transient power losses represent here a challenge. The proposed average model wishes to take care of the power switches' non-linear behaviour. An approximation is introduced to substitute the real current and voltage waveforms by ideal signals to enable the formal computation in step 6 of the algorithm. The real buck architecture is taken as an example (Fig. 16(a)). The initial bond graph to be averaged is pictured in Fig. 16(b).

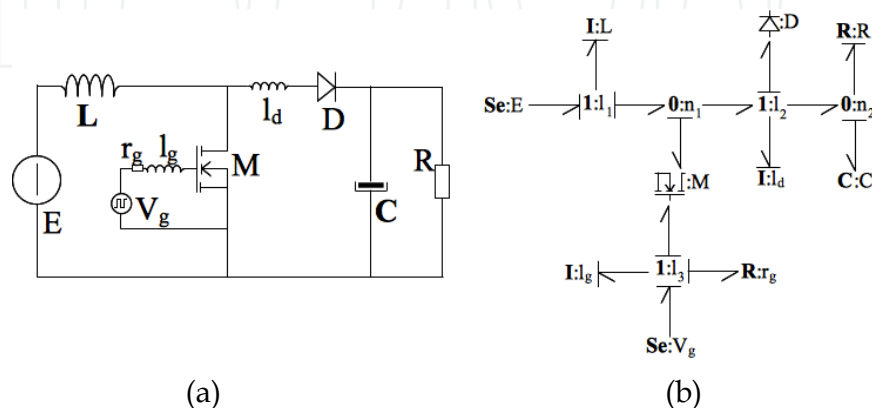


Fig. 16. Real buck converter (a) and related bond graph (b)

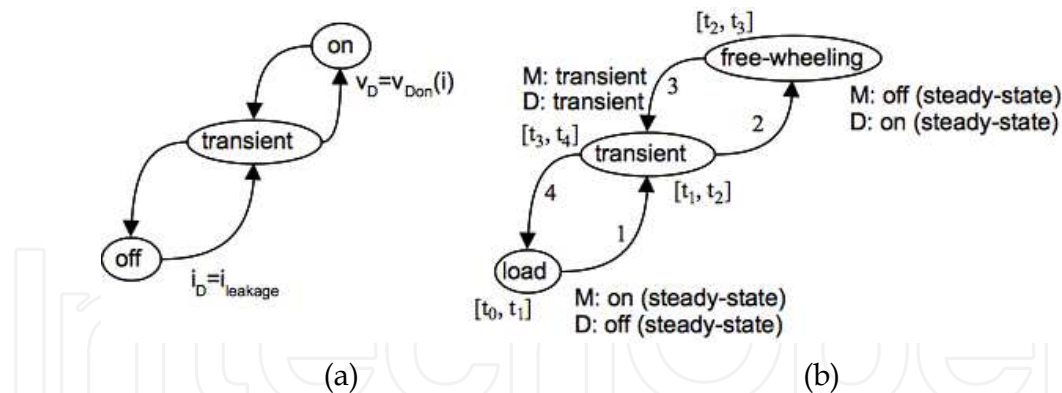


Fig. 17. Petri net of the power diode behaviour (a) and behaviour of the buck converter in Fig. 16(a) in continuous conduction mode (b)

The MOSFET model in Equation 1 is considered and the model in Equation 2 for the power diode. The behaviour of the power switches is pictured in Fig. 17(a) that leads to the buck converter Petri Net of states in Fig. 17(b) for the continuous conduction mode. The algorithm yields the simplified bond graph in Fig. 18. The input variables are  $I_1$  and  $V_2$ , and the output variables are  $v_1$  and  $i_2$ . The variable  $v_1$  is related to the MOSFET drain-source voltage while the output variable  $i_2$  is related to the diode current. According to the sequence in Fig. 17(b), the step 6 of the algorithm requires the computation of the following average values:

$$\begin{cases} \langle i_2 \rangle = \frac{1}{T_S} \left[ \int_{t_0}^{t_1} v_{DSon}(I_1) dt + \int_{t_1}^{t_2} v_{DS}(t) dt + \int_{t_2}^{t_3} (V_2 + v_{Don}(I_1)) dt + \int_{t_3}^{t_4} v_{DS}(t) dt \right] \\ \langle v_1 \rangle = \frac{1}{T_S} \left[ \int_{t_1}^{t_2} i_D(t) dt + \int_{t_2}^{t_3} I_1 dt + \int_{t_3}^{t_4} i_D(t) dt \right] \end{cases} \quad (5)$$

The proposed method is to substitute ideal signals to  $v_{DS}(t)$  and  $i_D(t)$  according to Fig. 18(b) and 18(c) respectively. Integrals of the real waveform and the ideal signal must be equal to lead to the same contribution in Equation (4). Virtual delays,  $\delta_{v_{DS}}^{off}$ ,  $\delta_{v_{DS}}^{on}$ ,  $\delta_{i_D}^{off}$  and  $\delta_{i_D}^{on}$  are introduced that depend on the switching block input variables and the circuit parasitic devices. Tabulation of virtual delay values may be measured or simulated.

The ideal signals and the virtual delays lead to the switching block average model in Equation (6). The bond graph in Fig. 19 is derived. The MTF element represents the average model of the ideal buck converter and the non linearities are reported in the two dissipative elements RS.

$$\begin{cases} \langle i_2 \rangle = I_1 \cdot \left[ \rho + \frac{\delta_{i_D}^{off} - \delta_{i_D}^{on}}{T_S} \right] \\ \langle v_1 \rangle = (V_2 - v_{DSon}) \cdot \left[ \rho - \frac{\delta_{v_{DS}}^{off} - \delta_{v_{DS}}^{on}}{T_S} \right] - v_{DSon} \cdot \left[ 1 - \rho + \frac{\delta_{v_{DS}}^{off} - \delta_{v_{DS}}^{on}}{T_S} \right] \end{cases} \quad (6)$$

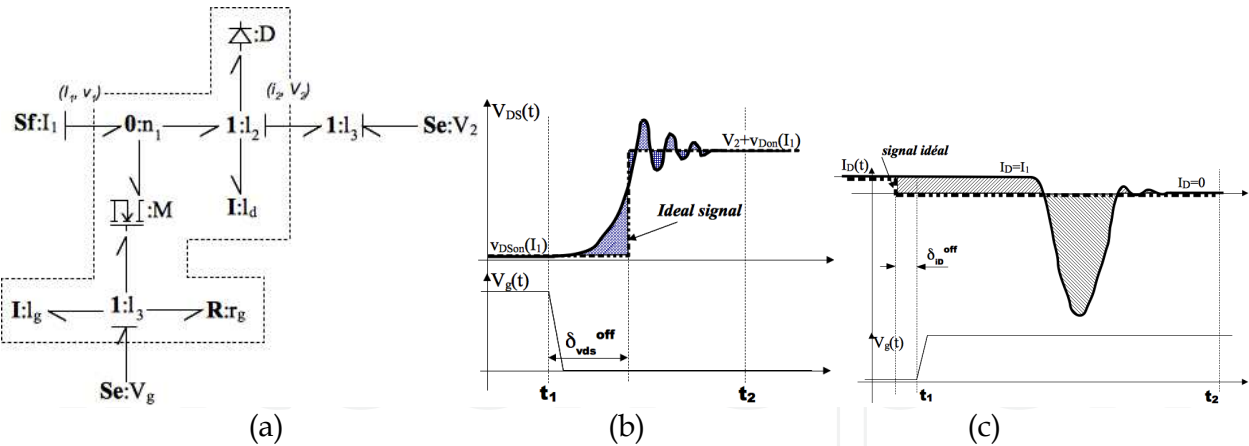


Fig. 18. Simplified bond graph (a) and ideal signal for the MOSFET drain voltage (b) and the diode current (c)

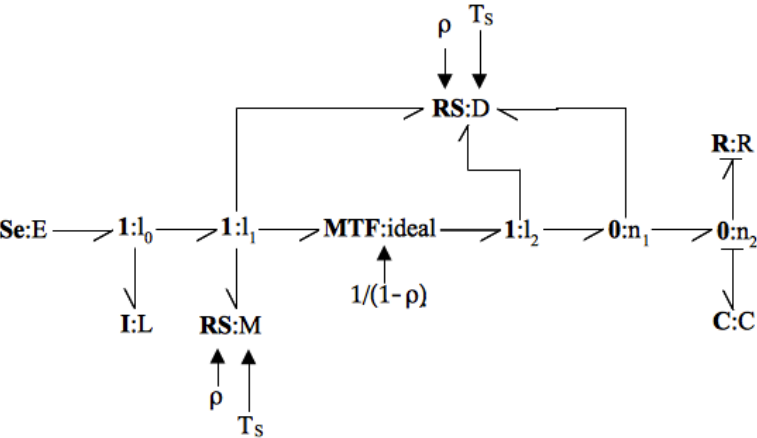


Fig. 19. Average model of the real buck converter in continuous conduction mode.

Many papers have been published to propose formal approximate waveforms for the current and voltages of power switches during transient. The switching power losses can then be calculated in a formal manner. Unfortunately the current and voltage waveforms depend on too many parameters to enable a valid approximation. The substitution proposed here above offers a practical advantage. The same idea of tabulation depending on the switching block parameters has been experimented for the power losses (Allard, 2001), (Ammous, 1998, 2000).

The system in Fig. 20 includes the here above buck converter that feeds a motor fan. The goal of an electro-thermal simulation is to provide an estimation of the power device self-heating behaviour on a long-term duration. This type of simulation requires the average model of the converter including losses. The losses are carried out with RS elements with at least a thermal bond. All thermal bonds are to be connected to a compact model of the system thermal network (like the thermal substrate in Fig. 20). A fast simulation gives results as in Fig. 21 that have been verified experimentally. The left figure compares an accurate device-level simulation of the buck converter to the ideal average model like in Fig. 12 and the buck converter non-ideal average model in Fig. 19. The right figure shows the start-up of the motor fan and the self-heating of the power devices.

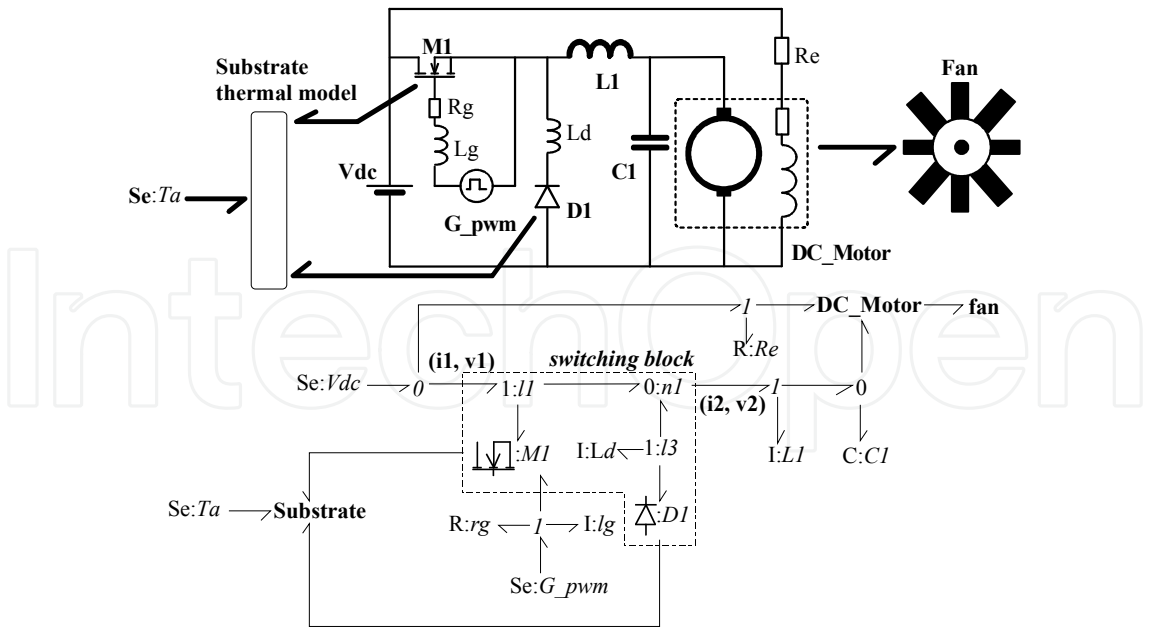


Fig. 20. Example of electro-thermal system

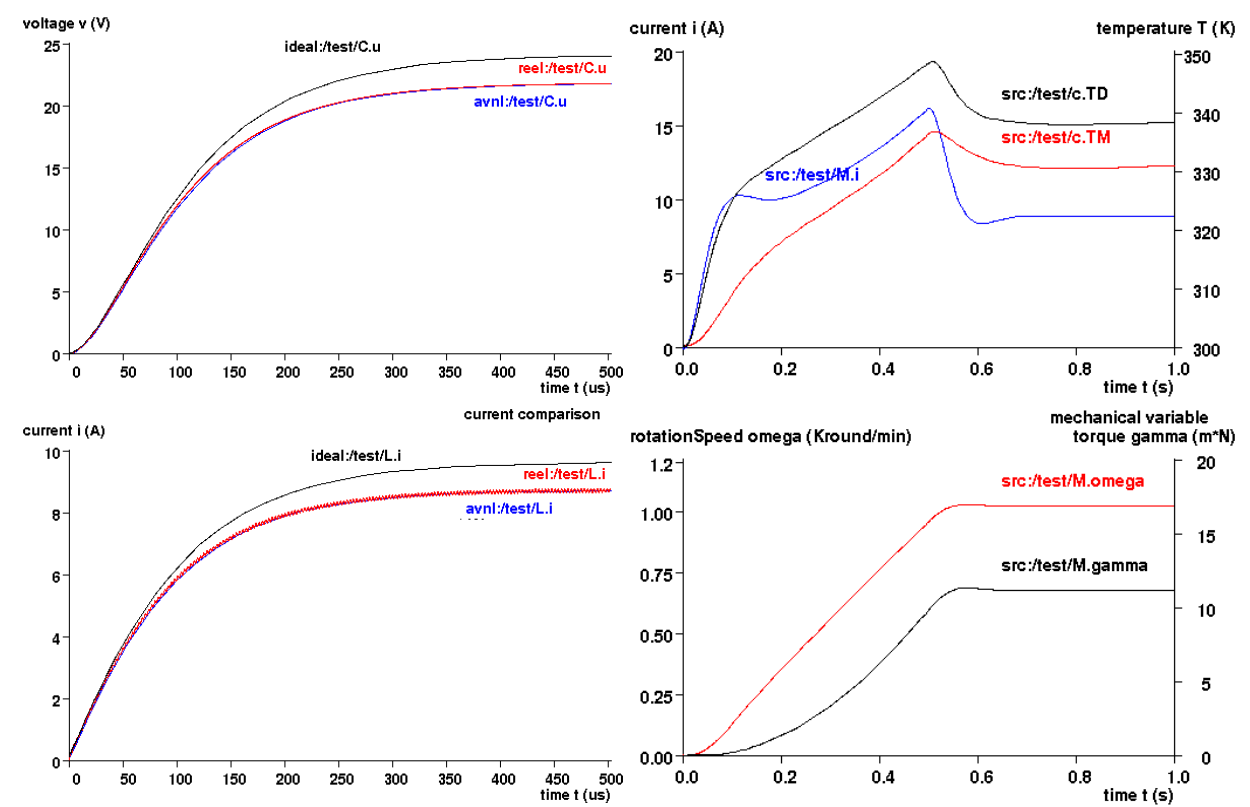


Fig. 21. Example of electro-thermal simulation.

7. Conclusion

This chapter has introduced the interests of compact models for system-level analyses of mechatronic products. Regarding the power converters, the compact models are called

average models and a systematic method has been detailed for their building. A simple example is presented at the end. The idea of ideal signals and look-up table of quantities has been applied to take care of EMI contributions.

Bond graphs have been used to build compact models of thermal system behaviour. This kind of compact model appears as the previous ones in the form of state-space models. VHDL-AMS is one example of language to implement easily the state-space models into a system simulator.

## 8. Annex A: Synthetic presentation of Bond Graphs and related graphical conventions

Bond Graphs is the name given to a framework for the unified modelling of the dynamics of multi-disciplinary systems. It is widely accepted in mechatronic industries like car manufacturers (Radcliffe, 1971), (Margolis, 1974), (Merzouki, 2007). The formalization of the bond graphs as known today is the results by Henry Painter (Painter, 1961). A popular introductory textbook is (Karnopp & Rosenberg, 1975). A rather complete bibliography may be found in (Bosand & Breedweld, 1985).

The First Law of Thermodynamics rules the evolution of a system internal energy that is balanced by heat transfer and external work energy transfer. This Law implies the continuity of energy with respect to time. The Bond Graphs assume also the continuum of micro-systems in the analysis of an engineering system. It is a lumped approach. Energy is then considered locally. Energy then flows into a system with identified boundaries. The system analyses are then valid only within these boundaries. The micro-systems' models are concepts or idealised descriptions of physical phenomena, which are recognised as the dominating behaviour in components (tangible system parts). The Bond Graph framework is a living tool where many ideas have been added since more than 50 years to simplify the modelling approach of dynamic systems. The topic is here to describe the basics of representation and the elementary component (i.e. simple concepts).

### 8.1 Flow and effort variables

The energy flow between two sub-systems inside the boundary-limited system is carried by a flow of particles, such as mass particles (solid, liquid, gas), electrons and holes, photons, phonons... The Bond Graph framework represents graphically this energy flow as in Fig. 22. The sub-systems A and B are connected through energy ports. In electrical domain, the energy ports are the pins of the devices. The half-arrow indicates the energy flow, directed from A to B.

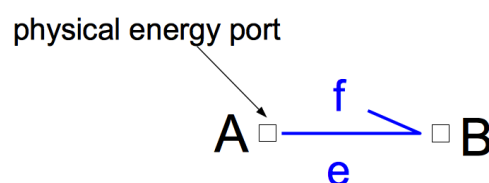


Fig. 22. Graphical representation of an energy exchange between two sub-systems.

The Onsager’s theorem<sup>3</sup> has established that the instantaneous power,  $p$ , characterizing the energy flow is the product of a flow variable,  $f$ , related to the flow of particles,  $f$ , by an effort variable,  $e$  (Equation 7).

$$P=f.e$$

(7)

The flow variable is an extensive variable whereas the effort variable,  $e$ , is an intensive variable. Table 4 gives a list of the effort and flow variables in the main physical domains. The graphical convention in Fig. 22 is to write the flow variable on the same side as the half-arrow and the effort variable on the other side. Referring to VHDL-AMS, the energy flow between two devices is defined by the connection of ‘terminals’. Quantities of branch are defined such as ‘through quantities’ and ‘across quantities’. The latter quantities may be chosen in essence similar to the flow variables and effort variables respectively.

Domain	Flow	Effort
Electrical	Current, $i$	Voltage, $v$
Translation	Velocity, $v$	Force, $f$
Rotation	Rotational speed, $\omega$	Torque, $\Gamma$
Hydraulic	Volume flow, $d$	Pressure, $p$
Thermal	Entropy flow, $S$	Temperature , $t$

Table 4. (effort, flow) couples in main physical domains

8.2 Bond Graph linear elements

A Bond Graph of a system is made of sub-systems that can be hierarchically subdivided into elementary components. In a first approach, it has been demonstrated that linear systems can be represented by the components in Table 5 (Breedveld, 1981). The C-element stores potential energy and its state-space model is given in Equation 8 where  $x$  is the state-variable.

Energy behaviour	Energetic	Entropic	Creator	None
Storage	C, I			
Irreversible		R, Rs		
Source			Se, Sf	
Constraint				0, 1, TF, MTF, GY, MGY

Table 5. Elements of a linear bond graphs

$$\begin{cases} \frac{dx}{dt} = f \\ e = \kappa(x) = x / C \end{cases}$$

(8)

An electrical capacitor takes the electrical charge,  $Q$ , as the state variable. The I-element in Table 5 is the self-inductor in electrical domain or the inertia in mechanical domain. The R-element is the energy dissipator. This element defines a resistor but also friction or Eddy current effect. The entropic RS-element is a two-port element that transforms the energy into heat (Fig. 23). The entropy flow ( $\dot{S}$  or  $f_s$ ) is the flow variable in the thermal domain is given

<sup>3</sup> Lars Onsager (November 27, 1903 - October 5, 1976). Valid in the case of thermodynamic equilibrium but extended to the case of resonable internal energy



by Equation 9. For convenience, the entropy flow is denoted  $f_s$ . The Second Law of Thermodynamics imposes that  $f_s$  is strictly positive.

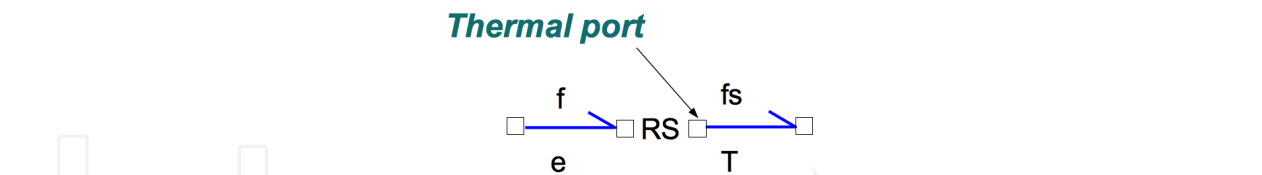


Fig. 23. Two-port, entropic element (RS)

$$f \cdot e = R \cdot f^2 = \dot{S} \cdot T = f_s \cdot T \tag{9}$$

It is said in introduction of this chapter that a system which analysis is considered here, is a limited by boundaries (from geometrical and energetic point of view). The outside world of the system is generally represented by sources: sources of effort,  $S_e$ , or sources of flow,  $S_f$ . The waveform of the source flow or effort may be of various types (continuous, harmonic). The elements of the system are linked so that they either share a flow of particles or an effort. Two elements are introduced to represent these connection types (Fig. 24). The so-called junction 1 connects the elements that share the same flow variable. It is equivalent to an electrical loop in electrical domain. The 0-junction connects the elements that share the same effort variable. It is equivalent to an electrical node in electrical domain or an iso-thermal connexion in thermal domain.

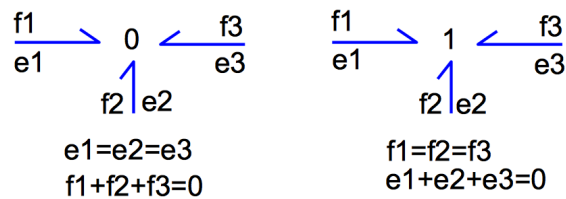


Fig. 24. Representation of junctions (case of 3-ports junctions)

Other constraint elements have been introduced along with junctions to describe other energy transfer and transformation. These constraint elements do not store energy, do not dissipate energy and evidently do not create energy. The most popular element is the transformer, representing the ideal gearbox, an electrical transformer or a pulley. The energy is transformed at equal instantaneous power. The transformer ratio may be different than one as represented in Fig. 25.

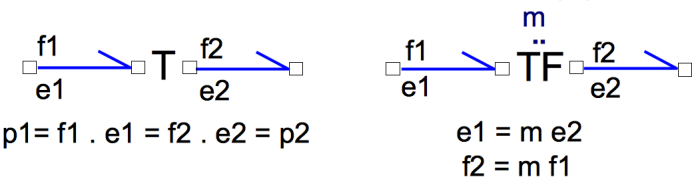


Fig. 25. Transformer elements

The mechanical gyroscope or the electrical coil introduce one final type of energy transformation between flow and effort variables. The gyrator-element has been introduced to take care of this particular energy exchange (Fig. 26). As an example, the electrical coil

model represents the electrical energy transformation into magnetic energy. In the magnetic domain, the flow variable is the derivative of the magnetic flux,  $\lambda=d\Phi/dt$ , and the effort variable is the magneto-motive force,  $F$ . The gyrator element is the natural representation for the following equations:  $v=N.\lambda$  and  $F=N.i$  where  $v$  and  $i$  are respectively the effort and flow variables of the electrical port and  $F$  and  $\lambda$  respectively the effort and flow variables of the magnetic port.

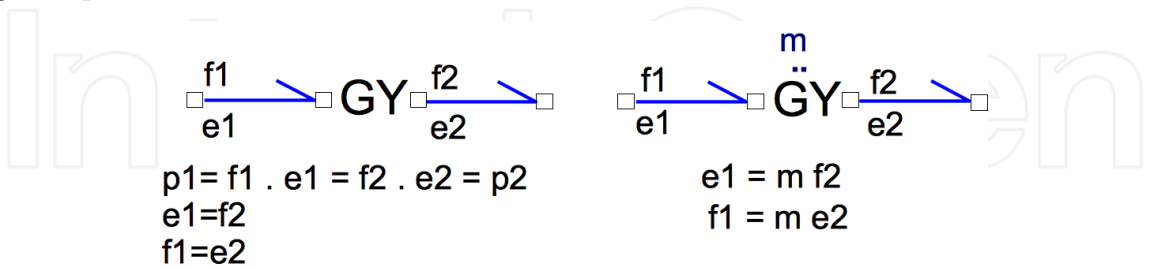


Fig. 26. Representation of the gyrator-element

The transformation ratio of the transformer, TF and the gyrator, GY, may be varying with time. In this case the elements are respectively denoted MTF and MGY but the constitutive equations remain similar.

8.3 Building a bond graph model

A large number of algorithms exist to build a Bond Graph from a pragmatic representation of a system. They are out of the scope of this chapter. Some algorithms deal with the construction of a bond graph from a Kirchhof representation of an electrical circuit (Karnopp, 1990). An advanced algorithm is detailed here after. This algorithm targets the simplification of complex Kirchhof networks. Basically all the nodes of the circuit are transformed into 0-junctions and rules are proposed to simplify the obtained brute bond graph:

1. Replace each component by the bond graph equivalent element and place a 1-junction at each port of each component.
2. Place a 0-junction between two earlier nodes. Respect the current orientation convention with the half-arrow orientation (Fig. 27).
3. Eliminate one 0-junction and the related half-arrow.
4. Simplify the resulting bond graph:
  - a. Eliminate the two-port, well-oriented junctions
  - b. Contract into one junction all linked junctions of the same nature
  - c. Eliminate the loop between 0- and 1-junctions
  - d. Simplify the association of 0-1-0-1 or 1-0-1-0 junctions
  - e. Experiment further simplification by inverting the half-arrow to an internal junction

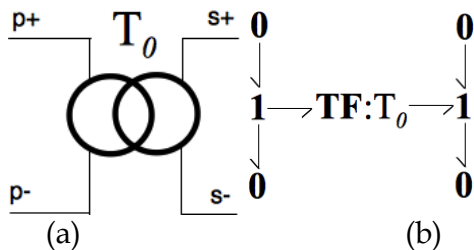


Fig. 27. Application of steps 1 and 2 of the algorithm. Redrawing of a transformer (a) into a bond graph equivalent (b)

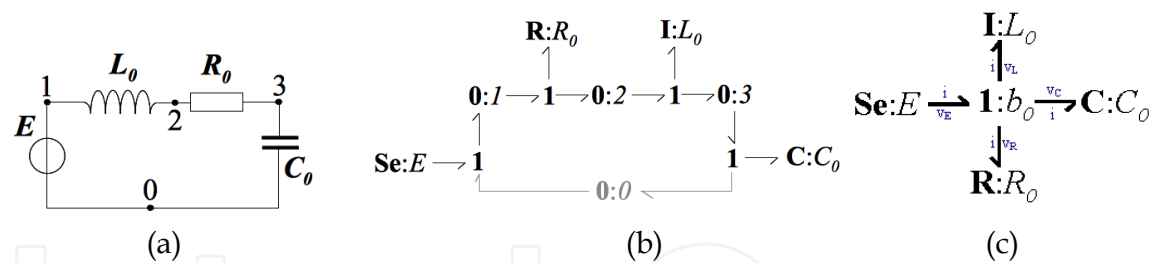


Fig. 28. Application of the algorithm to a simple circuit (a). Bond graphs after step 3 (b) and final bond graph (c).

9. Annex B: Synthetic presentation of the original causality analysis method

Causality or cause-to-effect relation is a philosophical concept since Spinoza in 1670. Physical systems verify that any phenomenon considered as a cause emerges due to another phenomenon considered as the cause and a delay appears between the effect and the caused. Classical mechanics, Maxwell equations or any state-space model verifies this rule, generally implicit.

The causality in the bond graph framework targets a model of the system at hand as an Ordinary Differential Equation. In a state space model like  $\dot{x} = G(x, t)$ , the Cauchy-Lipschitz theorem indicates that there is one solution given an initial condition if the function  $G$  is continuously derivable. It is mostly the case for physical systems. A so-called causal bond graph will then be described as an ODE. A non-causal bond graph will be described as a Differential and Algebraic Equation. The index theory of DAE indicates that only a subset of DAEs describe a deterministic system, i.e. enables a coherent simulation like an ODE (Lakner, 2008).

9.1 Causality of bonds

A bond graph element is meant to influence the system whether by the flow variable or the effort variable. The causality of an energy bond is the indication of the latter preference. The vertical stroke in Fig. 29 indicates that the element A dictates the value of the flow variable in the energy bond to the element B. Conversely the element B dictates the effort variable. It is the case of a causal bond. If both elements dictate the same variable, the causal representation is not possible and the bond is said non-causal: it is a physical impossibility like connecting in series two source of electrical current. Table 6 gives the causality graphical representation of the main bond graph elements. The column called “formal causality analysis” is related to section 3 of this chapter.

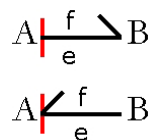


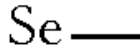







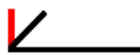




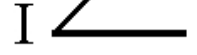








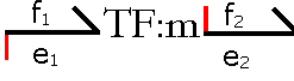
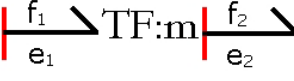
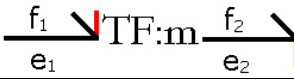
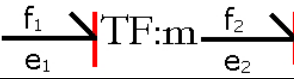


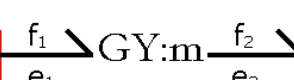

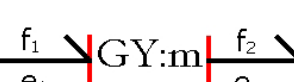
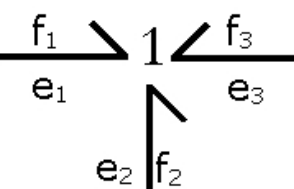
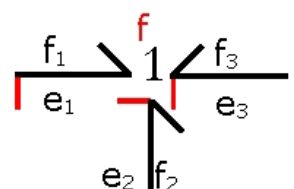
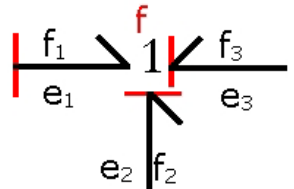


Fig. 29. Causality of an energy bond

If all the bonds of a given bond graph receive a consistent causal stroke, then the bond graph is said causal, i.e. the list of model equations is an ODE. Moreover an explicit list of equations is obtained in opposition of the implicit equation set that the Nodal Analysis Method exhibits in popular circuit simulator like Spice.

symbol	brute	Formal Causality Analysis	Original Causality
Se	Se 	Se 	Se 
Sf	Sf 	Sf 	Sf 
C in integral causality $\dot{x} = f, e = \varphi(x)$	C 	C 	C 
C in derivative causality <sup>4</sup> $f = \frac{\partial x}{\partial \varphi} \dot{e}$	C 	C 	C 
I in integral causality $\dot{x} = e, f = \varphi(x)$	I 	I 	I 
I in derivative causality $e = \frac{\partial x}{\partial \varphi} \dot{f}$	I 	I 	I 
R	R 	R 	R 
		R 	R 
TF or MTF			
			
GY or MGY			
			
1-junction			

<sup>4</sup> The derivative causality eliminates the state-space variables and leaves a DAE. It is a less favorable case than the ODE (integral causality)

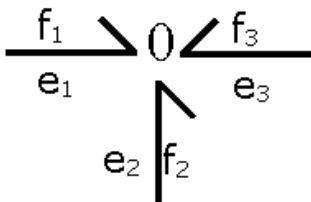
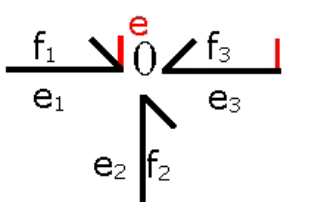
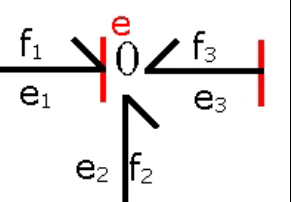
symbol	brute	Formal Causality Analysis	Original Causality
0-junction			

Table 6. Causality of bond graph elementary components

The causality of the bond graph in Fig. 28(c) is given in Fig. 30 along with the list of equations that is an ODE. An example of non-causal bond graph is given in section 3 of the chapter.

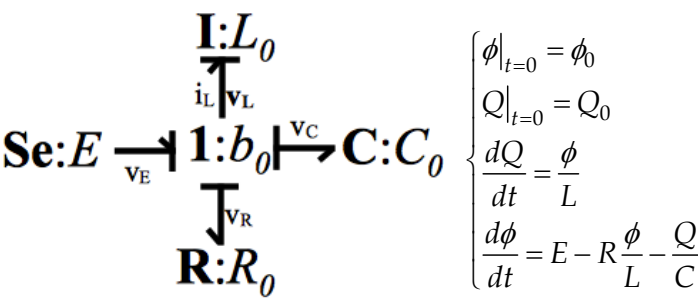


Fig. 30. Causality of the bond graph in Fig. 28(c) and associated equations

10. References

Allard, B., Morel, H., Ammous, A., Ghedira, S. (1997). Extension of Causality Analysis to Bond Graphs Including State-Space Models, *Proceedings of Society for Computer Simulation, Simulation Series*, Vol. 29, No. 1, pp. 72-78

Allard, B., Morel, H., Lautier, Ph., Retif, J.M. (1997). Bond Graphs for averaged Modeling of Power Electronic Converter, *Proceedings of Society for Computer Simulation, Simulation Series*, Vol. 29, No. 1, pp. 201-206.

Allard, B., Morel, H., Ghedira, S., Ammous. A. (1999). Building Advanced Averaged Models of Power Converters from Switched Bond Graph Representation, *Proceedings of Society for Computer Simulation, Simulation Series*, Vol. 31, No. 1, pp. 331-338.

Allard, B., Bergogne, D., Morel. H. (2001). Experimentally verified electro-thermal simulation of power converters, *Proceedings of SCS Publishing Editor, Simulation Series*, Vol. 33, No. 1, pp. 191-198.

Ammous, K., Allard, B., Morel. H. (2003). Switching-cell as a converter core-representation for analysis, *Proceedings of SCS Publishing Editor, Simulation Series*, Vol. 35, No. 2, pp. 72-78

Allard, B., Morel, H. (1998). Transient Temperature Measurements and Modeling of IGBT's Under Short-Circuit, *IEEE Transactions on Power Electronics*, Vol. 13, No. 1, pp. 12-25.

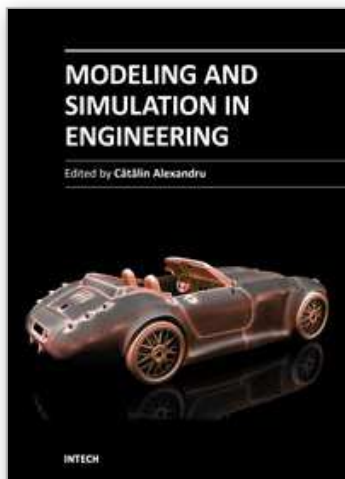
Ammous, A, Ammous, K., Morel, H., Allard, B., Bergogne, D., Sellami, F., Chante, J.P. (2000). Electrothermal Modeling of the IGBT's: Application to Short Circuit Condition, *IEEE Transactions on Power Electronics*, Vol. 15, No. 4, pp. 778-790.

- Ben-Yaakov, S., Wulich, D., Polivka, W.M. (1995). Resolution of an averaging paradox in the analysis of switched-mode dc-dc converters. *IEEE Transactions on Aerospace Electronic Systems*, Vol. 30, N°2, pp. 626-632.
- Bosand, A. M., Breedveld, P.C. (1985). Update of the Bond Graph Bibliography, In *University of Twente*, 20.06.2011, Available from <http://doc.utwente.nl/69379/1/Bos85update.pdf>
- Breedveld, P.C. (1981). *Thermodynamic bond graphs: a new synthesis*, International Journal of Modelling and Simulation, Vol. 1, No. 1, pp. 57-61.
- Cùk, S., Middlebrook, R.D. (1977). A general unified approach to modeling switching DC-to-DC converters in discontinuous conduction mode, *Proceedings of IEEE Power Electronics Specialists Conference*, pp.36-57.
- Karnopp, D.C., Rosenberg, R.C. (1975). *System dynamics, a unified approach*, Wiley, New-York
- Karnopp, D.C., Margolis, D.L., Rosenberg, R.C. (1990). *System dynamics: a unified approach*, (2nd edition), Wiley-Interscience, New-York.
- Krein, P.T., Bentsman, J., Bass, R.M., Lesieutre, B.C. (1990). On the use of averaging for the analysis of power electronics systems. *IEEE Transactions on Power Electronics*, Vol. 5, No. 2, pp. 182-190.
- Lai, Y.M., Tse, C.K., Mehta, P. (1995). A computer method for the formulation of averaged models for dc/dc power converter circuits. *Journal of Circuits, Systems and Computer*, Vol. 5, No 3, pp. 373-391.
- Lakner, P.R. (2008). Lumped Parameter Model Analysis, In *University of Queensland Hungarian Academy of Sciences*, 20.06.2011, Available from [www.dcs.vein.hu/lakner/oktatas/modellezes/chap5b.ppt](http://www.dcs.vein.hu/lakner/oktatas/modellezes/chap5b.ppt)
- Lee, Y.S. (1985). A systematic and unified approach to modeling switches in switch-mode power supplies. *IEEE Transactions on Industrial Electronics*, Vol. 32, pp. 445-448.
- Maksimovic, D. (1998). Automated small-signal analysis of switching converters using general purpose time-domain simulator, *Proceedings of IEEE Applied Power Electronics Conference and Exposition*, pp. 357-362.
- Margolis, D.L., Tylee, J.L. (1974). Bond graph modelling techniques applied to nonlinear primary and secondary suspensions for high speed ground transportation vehicles, *Proceedings of Simulation Council Series*, Vol. 4, No. 2, pp. 104-131.
- Merzouki, R., Ould-Bouamama, B., Djeziri, M.A., Bouteldja, M. (2007). Modelling and estimation of tire-road longitudinal impact efforts using bond graph approach. *Elsevier Mechatronics*, No. 17, pp. 93-108, doi:10.1016/j.mechatronics.2006.11.001
- Middlebrook, R.D., Cùk, S. (1976). A general unified approach to modeling switching converters, *Proceedings of IEEE Power Electronics Specialists Conference*, pp. 18-34.
- Morel, H., Allard, B., Brevet, O., We, M., Elomari, H., Ammous, K. (2001). Modified nodal approach versus causality analysis, *Proceedings of SCS Publishing Editor, Simulation Series*, Vol. 33, No. 1, pp. 85-90.
- Morel, H., Allard, B., Elomari, H., Ammous, K., Bergogne, D., Ammous, A. (2001). Causality Analysis and State Initialization, *SCS Publishing Editor, Simulation Series*, Vol. 33, No.1, January, pp. 91-97.
- Olivier, J.A., Cobos, J.A., Uceda, J., Rascon, M., Quinones, C. (2000). Systematic approach for developing large-signal averaged models of multi-output PWM converters, *Proceedings of IEEE Power Electronics Specialists Conference*, pp. 696-701.



- Painter, H. M. (1961). *Analysis and Design of engineering systems*, MIT Press, Cambridge, Mass.
- Pechoux, F., Allard, B., Lallement, C., Vachoux, A., Morel, H. (2005). Modeling and simulation of multi-discipline systems using bond graphs and VHDL-AMS, *Proceedings of SCS Publishing Editor, Simulation Series*, Vol. 37, No. 1, pp. 149-161.
- Radcliffe, C.J., Karnopp, D.C. (1971), Simulation of nonlinear air cushion vehicle dynamics using bond graph techniques, *Proceedings of Summer Computer Simulation Conference*, Board of Simulation Conference, 5975 Broadway, Denver, Colo., pp. 550-558.
- Sanders, S., Noworolski, J., Liu, X.Z., Verghese G.C. (1991). Generalized averaging method of power conversion circuits. *IEEE Transactions on Power Electronics*, Vol. 6, No. 2, pp. 251-258.
- Smedley, K., Cuk, S. (1994). Switching flow graph nonlinear modeling technique. *IEEE Transactions on Power Electronics*, Vol. 9, No. 4, pp. 405-413.
- Xu, J., Lee, C.Q. (1998). A unified averaging technique for the modeling of quasi-resonant converters. *IEEE Transactions on Power Electronics*, Vol. 13, No. 3, pp. 556-563.

IntechOpen



## **Modeling and Simulation in Engineering**

Edited by Prof. Catalin Alexandru

ISBN 978-953-51-0012-6

Hard cover, 298 pages

**Publisher** InTech

**Published online** 07, March, 2012

**Published in print edition** March, 2012

This book provides an open platform to establish and share knowledge developed by scholars, scientists, and engineers from all over the world, about various applications of the modeling and simulation in the design process of products, in various engineering fields. The book consists of 12 chapters arranged in two sections (3D Modeling and Virtual Prototyping), reflecting the multidimensionality of applications related to modeling and simulation. Some of the most recent modeling and simulation techniques, as well as some of the most accurate and sophisticated software in treating complex systems, are applied. All the original contributions in this book are joined by the basic principle of a successful modeling and simulation process: as complex as necessary, and as simple as possible. The idea is to manipulate the simplifying assumptions in a way that reduces the complexity of the model (in order to make a real-time simulation), but without altering the precision of the results.

### **How to reference**

In order to correctly reference this scholarly work, feel free to copy and paste the following:

Bruno Allard and Hervé Morel (2012). Analytical Compact Models, Modeling and Simulation in Engineering, Prof. Catalin Alexandru (Ed.), ISBN: 978-953-51-0012-6, InTech, Available from:  
<http://www.intechopen.com/books/modeling-and-simulation-in-engineering/analytical-compact-models>

**INTECH**  
open science | open minds

### **InTech Europe**

University Campus STeP Ri  
Slavka Krautzeka 83/A  
51000 Rijeka, Croatia  
Phone: +385 (51) 770 447  
Fax: +385 (51) 686 166  
[www.intechopen.com](http://www.intechopen.com)

### **InTech China**

Unit 405, Office Block, Hotel Equatorial Shanghai  
No.65, Yan An Road (West), Shanghai, 200040, China  
中国上海市延安西路65号上海国际贵都大饭店办公楼405单元  
Phone: +86-21-62489820  
Fax: +86-21-62489821

© 2012 The Author(s). Licensee IntechOpen. This is an open access article distributed under the terms of the [Creative Commons Attribution 3.0 License](https://creativecommons.org/licenses/by/3.0/), which permits unrestricted use, distribution, and reproduction in any medium, provided the original work is properly cited.

IntechOpen

IntechOpen